reducing agent. Because of the interference of TPA derivatives, our potential calibration with Fc/Fc^+ couple may not be very accurate either, which leaves little room for accommodating the contradictory results.

In summary, a stable and electrochemically reversible product can be voltammetrically detected after TPA is anodically oxidized in acetonitrile. Although it is not yet certain whether the observed redox wave is linked to the long-awaited reducing radical responsible for the generation of ECL excited state, the finding is an important clue to understanding the oxidation of TPA and ECL generation. With many follow-up reactions and short-lived intermediates, the anodic oxidation of aliphatic amines is very complicated. It is understandable that a convincing identification of the wave in question will need more experiments, which are under way in our laboratories and further results will be reported in due course.

Acknowledgements

K.B. and J.H. acknowledge the Fonds der Chemischen Industrie.

Keywords: amines · luminescence · electrochemistry · tripropylamine

[1] J. K. Leland, M. J. Powell, *J. Electrochem. Soc.* **1990**, *137*, 3127 – 3131.
[2] Y. Zu, A. J. Bard, *Anal. Chem.* **2000**, *72*, 3223 – 3232.
[3] F. Kanoufi, Y. Zu, Y., A. J. Bard, *J. Phys. Chem. B* **2001**, *105*, 210 – 216.
[4] E. M. Gross, P. Pastore, R. M. Wightman, *J. Phys. Chem. B* **2001**, *105*, 8732 – 8738.
[5] W. Miao, J.-P. Choi, A. J. Bard, *J. Am. Chem. Soc.* **2002**, *124*, 14478 – 14485.
[6] G. F. Blackburn, H. P. Shah, J. H. Kenten, J. Leland, R. A. Kamin, J. Link, J. Peterman, M. J. Powell, A. Shah, D. B. Talley, S. K. Tyagi, E. Wilkins, T.-G. Wu, R. J. Massey, *Clin. Chem.* **1991**, *37/9*, 1534 – 1539.
[7] K. Erler, *Wien. Klin. Wochenschr.* **1998**, *110*, 5 – 10.
[8] P. J. Smith, C. K. Mann, *J. Org. Chem.* **1969**, *34*, 1821 – 1825.
[9] L. C. Portis, V. V. Bhat, C. K. Mann, *J. Org. Chem.* **1970**, *35*, 2175 – 2178.
[10] M. Zhou, J. Heinze, *J. Phys. Chem. B* **1999**, *103*, 8443 – 8450.
[11] H. Kiesele, *Anal. Chem*. **1981**, *53*, 1952 – 1954.
[12] A trace amount of oxygen in the solution can react with the reducing agent and result in the disappearance of the anodic wave.
[13] a) M. M. Richter, A. J. Bard, W. Kim, R. H. Schmehl, *Anal. Chem.*, **1998**, *70*, 310 – 318; b) M. Zhou, J. Roovers, *Macromolecules,* **2001**, *34*, 244 – 252.
[14] a) A redox potential of about -1.7 V vs. Ag/AgCl was estimated for the reducing radical in ref. [28] of the above ref. [5]. This estimation is based on ECL research of a series of organic systems. See ref. [14b]. A similar value was also estimated in ref. [14c]; b) R. Y. Lai, A. J. Bard, *J. Phys. Chem. A* **2003**, *107*, 3335 – 3340; c) K. Bhattacharyya, P. K. Das, *J. Phys. Chem. B* **1986**, *90*, 3987 – 3993.
[15] D. D. M. Wayner, D. J. McPhee, D. Griller, *J. Am. Chem. Soc.* **1988**, *110*, 132 – 137.
[16] a) The $E_{1/2}$ values for $[Ru(bpy)_3]^{3+}/[Ru(bpy)_3]^{2+*}$ couple were often reported and cited with respect to different reference electrodes in different electrolyte systems and there is confusion in the literatures. For example, the values of $E_{1/2} = -0.81$ V in acetonitrile vs. SCE, -0.81 V in acetonitrile vs. sodium saturated calomel electrode (SSCE) and -0.83 V in water vs. SCE were reported in ref.s [16b,c], [16d], and [16e], respectively. However, the values of -0.83 V vs. normal hydrogen electrode (NHE), -0.84 V vs. NHE, -0.85 V vs. NHE and -1.06 V vs. Ag/AgCl were used in ref.s [16f,g], [3], [16h], and [5]. The difference between two extreme values with respect to the same reference electrode is about 0.2 V. Here we cite the most negative value, used also in ref. [5]; b) C. R. Bock, T. J. Meyer, D. G. Whitten, *J. Am. Chem. Soc.* **1975**, *97*, 2909 – 2911; c) C. R. Bock, J. A. Connor, A. R. Gutierrez, T. J. Meyer, D. G. Whitten, B. P. Sullivan, J. K. Nagle, *J. Am. Chem. Soc.* **1979**, *101*, 4815 – 4824; d) C. P. Anderson, D. J. Salmon, T. J. Meyer, R. C. Young, *J. Am. Chem. Soc.* **1977**, *99*, 1980 – 1982; e) C. Creutz, N. Sutin, *Inorg. Chem.* **1976**, *15*, 496 – 499; f) A. Juris, M. T. Gandolfi, M. F. Manfrin, V. Balzani, *J. Am. Chem. Soc.* **1976**, *98*, 1047 – 1048; g) M. Kirch, J.- M. Lehn, J. P. Sauvage, *Helvetica Chimica Acta* **1979**, *62*, 1345 – 1383; h) S. Glazier, J. A. Barron, N. Morales, A. M. Ruschak, P. L. Houston, H. D. Abruña, *Macromolecules* **2003**, *36*, 1272 – 1278.

Received: June 17, 2003 [Z875]

Time-Resolved Second Harmonic Generation Near-Field Scanning Optical Microscopy

Richard D. Schaller, Justin C. Johnson, and Richard J. Saykally*[a]

Novel scanning probe microscopy (SPM) spectroscopic techniques are currently receiving much attention. The increasing number of spectroscopic techniques, when combined with the high spatial resolution that is attainable with SPM, makes it possible to probe a large range of material characteristics on the nanoscopic scale. The ability to probe samples on the nanoscale with femtosecond time resolution promises to increase our knowledge of nanoscale electronic devices and their dynamics.

Several time-resolved spectroscopic probes have recently been demonstrated in combination with SPM techniques. Ambrose et al.[1] as well as Xie and Dunn[2] and Trautman and Macklin[3] have performed fluorescence lifetime measurements in combination with near-field scanning optical microscopy (NSOM), and found that the excited-state lifetimes of emissive dye molecules were sensitive to the proximity of a metal-coated NSOM probe. This change in lifetime was explained in terms of energy transfer between the dye and the metal coating of the probe.[4] Transient linear reflectivity,[5, 6] transient transmissivity,[7] and transient absorption NSOM techniques have also been demonstrated.[8–10] Shigekawa and co-workers have also demonstrated transient conductivity scanning tunneling microscopy (STM) on a GaAs sample using resonant, femtosecond-pulse-width excitation.[11]

Time-resolved second harmonic generation (TRSHG) has been utilized in far-field measurements of changes in molecular orientation at interfaces,[12] in dynamic studies of carrier lifetimes in semiconductors,[13] and as a probe of coherent phonon relaxation.[14] The magnitude of the second-order induced polarization, $P^{(2)}$ produced in a sample (the square of which is equal to the magnitude of the detectable SHG signal) is proportional to the elements of a nonlinear susceptibility tensor

[a] *Professor R. J. Saykally, Dr. R. D. Schaller, J. C. Johnson*
Dept. of Chemistry, University of California
Berkeley, CA 94720 – 1460 (USA)
Fax: (+1) 510 – 642 – 8566
E-mail: saykally@uclink4.berkeley.edu

 DOI: 10.1002/cphc.200300907

($\chi_{ijk}^{(2)}$) and the square of the electric field (E) for an incident laser probe pulse at the fundamental frequency ω, where i, j, and k are laboratory coordinates, as described by Equation (1)

$$P_i^{(2)}(2\omega) = \chi_{ijk}^{(2)} E_j(\omega) E_k(\omega) \quad (1)$$

where $\chi^{(2)}$ is composed of resonant and nonresonant components that can be separately probed based upon the frequency of the probe pulse. In the TRSHG experiments that follow in which we study a polycrystalline ZnSe sample (a II-VI semiconductor), E is fixed in magnitude, but $\chi_{ijk}^{(2)}$ is caused to vary as a function of time, relative to a femtosecond pump pulse that creates a time-dependent population of carriers (N). For a nonresonant SHG probe, $\chi^{(2)}$ will change with time due to generation and relaxation of carriers, as well as due to any excitation-induced distortion of the crystal lattice. Resonant components of $\chi^{(2)}$, which we do not explore in this work, can be more complicated to interpret than nonresonant components in TRSHG experiments, as any pump-induced energy shifting of band energies will also cause detuning of the SHG resonance[15] to change with time. Furthermore, because TRSHG is sensitive to N^2, measured time constants are correspondingly faster (and more sensitive to N) than those observed using linear time-resolved techniques.

Here, we first describe TRSHG experiments performed in the far-field using both one- and two-photon sample excitation, in which we monitor the time-dependence of the sample SHG efficiency using a nonresonant probe pulse. Femtosecond laser pump pulses that are one- or two-photon resonant with the band gap of ZnSe excite carriers, which causes a time-dependent decrease in the second-order optical response ($\chi^{(2)}$) of the material. Next, with an understanding of the far-field TRSHG response of the sample, we performed near-field TRSHG experiments using two-photon sample excitation and collect the TRSHG signals using the nanoscopic fiber probe of an NSOM. In these novel measurements, we observe relaxation dynamics that are more similar to those measured in far-field experiments performed with one-photon excitation, which we attribute to an effect of limited NSOM depth of field.

Carrier dynamics in bulk ZnSe have been investigated previously. Wong and coworkers[16, 17] have performed photoluminescence upconversion (PLU) measurements on the band-edge emission of ZnSe following one-photon (with an energy of 3.1 eV) and two-photon (using two photons of 1.55 eV) excitation. In these experiments, which monitor the rate of radiative relaxation, one-photon excitation was observed to engender more rapid relaxation dynamics than did two-photon excitation. Because 3.1 eV photons only penetrate $\approx$100 nm[18] into ZnSe, which has a 2.7 eV band gap at 298 K,[19] in comparison to the near transparency of the sample to 1.55 eV, differences in the relaxation dynamics were attributed to the increased importance of surface recombination velocity on the carriers produced using the former excitation method. Mehendale et al.[20] have also studied the relaxation of hot electrons in ZnSe, which had been excited with 3.1 eV photons, using transient reflectivity. In that work, the sub-picosecond cooling times of hot electrons were measured for a sample of 160 nm thickness as a function of carrier density, and were found to be consistent with the successive emission of LO phonons.

A commercial NSOM system (TMmicroscopes, Lumina), which we have previously employed for other coherent nonlinear optical measurements,[21–25] was used for the near-field TRSHG measurements. The microscope uses a nonoptical, tuning fork shear-force feedback mechanism to maintain a constant tip-to-sample separation of $\approx$5–10 nm. Fiber optic probes with a $\approx$50 nm diameter tip were produced using standard chemical etching techniques[26] and were not metal-coated so as to avoid perturbation of the sample.[1–3, 27] The sample consisted of a polycrystalline disk (1 mm thick) of chemical-vapor-deposited (CVD) ZnSe with a grain size of $\approx$50 μm. The sample was washed extensively with methanol and dried under vacuum prior to experiments. All experiments were performed at room temperature.

The light source for the TRSHG experiments consisted of a home-built titanium:sapphire oscillator (800 nm, 480 mW, 30 fs, 88 MHz), which was used to seed a commercial (Spectra-Physics) chirped pulse amplifier (800 nm, 2.25 W, 80 fs, 1 kHz). This output was beamsplit 90:10, using 90% to pump a commercial (Quantronix, Topaz) superfluorescence optical parametric amplifier (OPA). The OPA was tuned to produce the electronically nonresonant fundamental probe pulse at 1.32 μm (4 μJ, 80 fs, 0.94 eV). The residual 10% of the amplifier output was used to provide electronic excitation of the CVD ZnSe sample. The 800 nm pulses were used after attenuation to excite the sample electronically via a two-photon absorption process. A BBO crystal was also used to frequency double the residual amplifier output so as to excite the sample via a one-photon process. Carrier densities using either method of sample excitation were on the order of 10^{17} cm^{-3}.

Whereas two separate experimental configurations were used, far- and near-field TRSHG measurements were conducted in a similar geometry, as described in Figure 1. Noise in the detected SHG signals, primarily due to shot-to-shot laser instabilities, was reduced using home-built, on-the-fly shot rejection electronics. Acceptance of a laser shot was determined by the response of a photodiode that monitored the probe pulse energy, which was the least stable of the laser pulses.

Under certain circumstances,[15] SHG can be implemented to selectively probe molecules that reside at interfaces. However, it is important to point out that the ZnSe crystal structure (zinc-blende) lacks inversion symmetry, such that detected SHG signals in this work will be dominated by a bulk contribution.[28] Moreover, while we do not demonstrate the spatial resolution of our SHG NSOM techniques here, we routinely observe optical spatial resolution of $\approx$100 nm in similar experiments.[21]

Figure 2 shows typical far-field TRSHG data obtained using (a) one- (3.1 eV) and (b) two-photon (2×1.55 eV = 3.1 eV) excitation of a CVD ZnSe sample, monitored using the non-electronically-resonant SHG probe pulse (fundamental = 0.94 eV, SHG = 1.88 eV). The dynamic responses of the sample to the two methods of excitation are clearly distinguishable. Both modes of excitation result in a very rapid initial decrease of the SHG efficiency that is approximately the far-field instrument response function ($\approx$120 fs) (shown in Figure 3 inset). The electronic

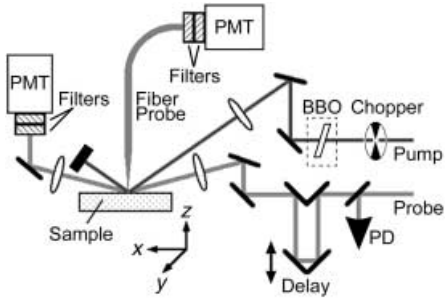

Figure 1. *Far- and near-field time-resolved SHG experiments. Far- and near-field TRSHG experimental setups were similar. P-polarized pump and probe pulses produced by an femtosecond Ti:sapphire laser and optical parametric amplifier operating at 1 kHz were incident upon the sample at 55° and 70° from normal, respectively, and were spatially overlapped on the sample surface. A photodiode (PD) was used to monitor pulse to pulse stability of the probe pulses and was also implemented for on-the-fly shot rejection. A synchronized chopper was used to reduce the frequency of the pump pulses to 500 Hz. Pulses centered at 800 nm were used to provide two-photon sample excitation or a BBO doubling crystal and two dichroic mirrors could be inserted into the pump beam path to provide one-photon excitation. Probe pulses at 1.32 μm were focused to a spot size that was half that of the pump spot size, such that a homogeneously excited region of the sample was probed. Timing of the probe pulse relative to the pump pulse was controlled with a computer controlled, motorized delay line. SHG photons produced in the sample were either collected with a collimating lens in the direction of the specular reflection of the probe pulse for far-field measurement or via an NSOM fiber probe held ≈ 5 nm from the sample surface in the center of the pump spot. Collected SHG photons were subsequently directed to two broad bandpass filters centered at 660 nm before detection by a Hamamatsu 3896 photomultiplier tube (PMT) biased at − 700 V (for far-field) or − 1000 V (for near-field), respectively. SHG NSOM signal levels were ≈ 5 – 15 photons/shot. Data points in far- and near-field TRSHG time traces represent the average of 800 and 1600 laser shots, respectively. TRSHG experiments performed for other non-electronically resonant probe wavelengths produced results similar to those presented.*

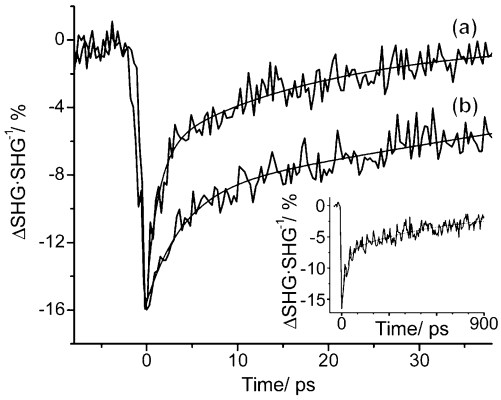

Figure 2. *Far-field time-resolved SHG. TRSHG time traces performed on a ZnSe sample using (a) one- (3.1 eV) and (b) two-photon (2 × 1.55 eV = 3.1 eV) sample excitation show significantly different relaxation dynamics, as monitored by a nonresonant probe pulse. While both modes of excitation result in a similar slow relaxation time constant on the nanosecond time scale (shown on a longer timescale using two-photon excitation in the inset), which is consistent with radiative carrier relaxation, one-photon excitation results in rapider initial carrier relaxation. This disparity in rates is attributed to differences in the penetration depth of the excitation photons, namely, above-band gap linear excitation penetrates only ≈ 100 nm into the sample whereas two-photon excitation penetrates entirely through the material. Therefore, the differences in rates are attributed to effects of surface-mediated relaxation and trapping processes.*

relaxation that follows using either means of excitation can be adequately described as a biexponential decay of the transients with a fast (ca. picoseconds) component, and a process that is orders of magnitude slower (shown on a longer timescale in Figure 2 as an inset). Relaxation occurs more quickly for excitation that results from linear excitation (Figure 2 a) than from the two-photon excited response (Figure 2 b).

Biexponential fits to the relaxation of the far-field TRSHG data are also shown in Figure 2. While both traces exhibit similar slow relaxation on the nanosecond timescale, which is consistent with previously measured radiative recombination rates for bulk ZnSe,[16, 17] the fast processes observed for each differ by a factor of three, with 1.6 ps (± 0.2) and 4.4 ps (± 0.6) time constants for one- and two-photon excitation, respectively. We attribute the time-dependent changes in SHG efficiency to the formation and relaxation of hot carriers with an initial 300 meV of excess energy in the semiconductive sample. The observed decrease in SHG efficiency following electronic sample excitation indicates that carriers act to reduce the nonlinear polarizability of the highly polar semiconductor.[20]

Using arguments made by Wong and co-workers,[16, 17] we interpret the observed differences in far-field TRSHG relaxation rates for the different means of sample excitation to be due to the differences in penetration depth of the incident excitation photons into the sample, as described above. The shallow penetration depth of the above band-gap 3.1 eV photons (≈ 100 nm) for the one-photon sample excitation results in a larger contribution of surface-mediated carrier relaxation processes. A reduced surface contribution to the carrier dynamics is observed for the two-photon method of excitation using 1.55 eV photons, as expected,[29, 30] as the below band-gap pump photons propagate entirely through the semiconductor, which thus reduces the relative surface contribution to TRSHG signals.

The fast relaxation component is likely a convolution of hot carrier cooling via LO phonon emission, which has been observed to be 400 – 700 fs in ZnSe, depending on generated carrier density,[20] and surface-mediated carrier relaxation and trapping. In comparison to PLU experiments, which measure the rate of radiative relaxation, TRSHG experiments are sensitive to the total carrier density, irrespective of relaxation pathway. Since one- and two-photon carrier excitations both deposit the same total amount of excess energy into the carriers, the hot-carrier cooling contribution to the TRSHG signals should be indistinguishable; this leaves differences in surface-mediated relaxation to account for the factor of three observed difference in relaxation time for the two methods of excitation.

Shown in Figure 3 is a reproducible TRSHG NSOM trace produced using two-photon excitation of the same ZnSe sample studied in the far-field and a non-electronically resonant SHG probe.[31] In similarity to the measured far-field dynamics, biexponential relaxation dynamics are observed, with the slow process occurring on the order of nanoseconds. The fast relaxation component observed in the near-field detected TRSHG signals is 2.1 ps (± 0.2). This result is significantly faster than the two-photon excited far-field TRSHG response, and is closer to the dynamics measured for far-field linear excitation.

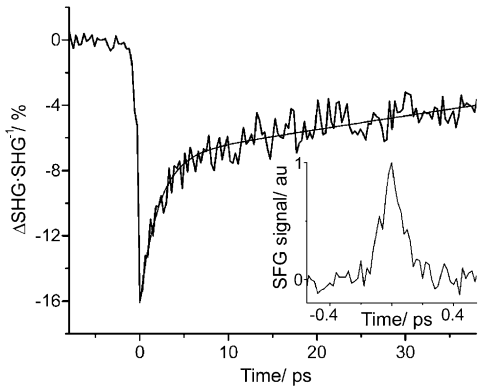

Figure 3. *Near-field detected TRSHG. The TRSHG response following two-photon sample excitation as monitored in the near-field relaxes faster than it does in similar far-field TRSHG experiments shown in Figure 2 (b). Although two-photon excitation penetrates entirely through the ZnSe sample, dynamics of carriers near the sample surface contribute more to the collected TRSHG NSOM signals due to the intrinsically shallow depth of field (ca. equal to the tip diameter, 50 nm).[35] The instrument response function of our TRSHG NSOM experiment (shown as an inset) was measured by detection of the sum frequency generation (SFG) cross correlation signal produced between the pump and probe pulses, which has a 120 fs FWHM.*

Such results were reproducible for many regions monitored on the sample.

We attribute the differences in the measured dynamics for two-photon excited TRSHG experiments performed in the far- and near-field to be related to the shallow depth of field effected by collection mode NSOM experiments. As the depth of field of oblique collection mode NSOM is comparable to the penetration depth of above band-gap excitation at 3.1 eV, carrier relaxation near the surface, which is faster than in the bulk, contributes more to the near-field detected TRSHG signals.

In conclusion, we have demonstrated the feasibility of TRSHG NSOM by studying ultrafast carrier dynamics in a II-VI semiconductor. We have measured the far- and near-field TRSHG response of ZnSe and observed faster carrier relaxation in far-field measurements with one-photon excitation than with two-photon excitation. In near-field experiments performed with two-photon excitation, we observe sample relaxation that is more similar to one-photon far-field TRSHG measurements, which we attribute to a characteristic of NSOM performance. Our initial investigations of spatial variation in the dynamics of TRSHG responses in ZnSe did not reveal any measurable differences, though we expect that improvements in signal-to-noise will show correlations with the heterogeneity that we have observed previously in static SHG and sum frequency generation (SFG) NSOM measurements.[21, 23] With such improvements, we expect that TRSHG NSOM will become a useful tool for the characterization of surface traps and defects in meso- and nanoscale materials and devices. It is expected that a longer timescale is needed for more sensitive characterization of trap states. The technique should eventually also be useful for the characterization of a wide range of sample properties, from ultrafast phase transitions[32] to changes in molecular orientation of adsorbed layers[12, 33, 34] with high spatial resolution.

We propose that TRSHG experiments performed on nanoscopic semiconductive materials will not exhibit the differences in dynamics observed here for one- versus two-photon excitation. Nanoscale materials, which have very large surface-to-bulk ratios, would not be expected to exhibit any differences in relaxation rates due to photoexcitation penetration depth. However, such materials would be expected to have faster initial relaxation rates (as measured by TRSHG), as surface-mediated relaxation of carriers will play a more important role than in bulk materials.

Acknowledgements

This work was supported by the Experimental Physical Chemistry Division of the National Science Foundation (CHE-9727302).

Keywords: nanotechnology · near-field microscopy · nonlinear optics · second harmonic generation · semiconductors · time-resolved spectroscopy

[1] W. P. Ambrose, P. M. Goodwin, J. C. Martin, R. A. Keller, *Science* **1994**, *265*, 364 – 367.
[2] X. S. Xie, R. C. Dunn, *Science* **1994**, *265*, 361 – 364.
[3] J. K. Trautman, J. J. Macklin, *Chem. Phys.* **1996**, *205*, 221 – 229.
[4] R. X. Bian, R. C. Dunn, X. S. Xie, P. T. Leung, *Phys. Rev. Lett.* **1995**, *75*, 4772 – 4775.
[5] J. Levy, V. Nikitin, J. M. Kikkawa, D. D. Awschalom, *J. Appl. Phys.* **1996**, *79*, 6095 – 6100.
[6] T. Guenther, C. Lienau, T. Elsaesser, M. Glanemann, V. M. Axt, T. Kuhn, S. Eshlaghi, A. D. Wieck, *Phys. Rev. Lett.* **2002**, *89*, 57 401 – 57 404.
[7] A. H. La Rosa, C. L. Jahncke, H. D. Hallen, *Proc. of the SPIE* **1995**, *2384*, 101 – 108.
[8] B. A. Nechay, U. Siegner, M. Achermann, F. Morier-Genoud, A. Schertel, U. Keller, *J. Microsc.* **1999**, *194*, 329 – 334.
[9] M. Acherman, B. A. Nechay, U. Siegner, A. Hartmann, D. Oberli, E. Kapon, U. Keller, *Appl. Phys. Lett.* **2000**, *76*, 2695 – 2697.
[10] A. A. Mikhailovsky, M. A. Petruska, L. Kuiru, M. I. Stockman, V. I. Klimov, *Optics Lett.* **2003**, *28*, 1686 – 1688.
[11] O. Takeuchi, R. Morita, M. Yamashita, H. Shigekawa, *Jpn. J. Appl. Phys. Part 1* **2002**, *41*, 4994 – 4997.
[12] A. V. Benderskii, K. B. Eisenthal, *J. Phys. Chem. B* **2000**, *104*, 11 723 – 11 728.
[13] F. Minami, Y. Mitsumori, S. Matsushita, *Phys. Stat. Sol. (B)* **1997**, *202*, 775 – 782.
[14] Y. M. Chang, L. Xu, H. W. K. Tom, *Phys. Rev. Lett.* **1997**, *78*, 4649 – 4952.
[15] Y. R. Shen, *The Principles of Nonlinear Optics*. **1984**, New York, Wiley.
[16] W. J. Peng, H. Wang, K. S. Wong, G. K. L. Wong, *QELS* **1996**, *10*, 55 – 56.
[17] H. Wang, K. S. Wong, B. A. Foreman, Z. Y. Yang, G. K. L. Wong, *J. Appl. Phys.* **1998**, *83*, 4773 – 4776.
[18] S. Adachi, T. Taguchi, *Phys. Rev. B* **1991**, *43*, 9569 – 9577.
[19] J. R. Chelikowsky, M. L. Cohen, *Phys. Rev. B* **1976**, *14*, 556 – 582.
[20] M. Mehendale, S. Sivananthan, W. A. Schroeder, *Appl. Phys. Lett.* **1997**, *71*, 1089 – 1091.
[21] R. D. Schaller, J. C. Johnson, K. R. Wilson, L. F. Lee, L. H. Haber, R. J. Saykally, *J. Phys. Chem. B* **2002**, *106*, 5143 – 5154.
[22] R. D. Schaller, C. Roth, D. H. Raulet, R. J. Saykally, *J. Phys. Chem. B* **2000**, *104*, 5217 – 5220.
[23] R. D. Schaller, R. J. Saykally, *Langmuir* **2001**, *17*, 2055 – 2058.
[24] J. C. Johnson, H. Yan, R. D. Schaller, P. B. Petersen, P. Yang, R. J. Saykally, *Nanolett.* **2002**, *2*, 279 – 283.
[25] R. D. Schaller, R. J. Saykally, Y. R. Shen, F. Lagugné-Labarthet, *Optics Lett.* **2003**, *28*, 1296 – 1298.
[26] P. Hoffmann, B. Dutoit, R. P. Salathe, *Ultramicroscopy* **1995**, *61*, 165 – 170.
[27] I. I. Smolyaninov, A. V. Zayats, C. C. Davis, *Phys. Rev. B* **1997**, *56*, 9290 – 9293.
[28] C. Yamada, T. Kimura, *Phys. Rev. B* **1994**, *49*, 14 372 – 14 381.
[29] The depth of field (DOF) for the two-photon excited, far-field TRSHG experiments will be dictated by the coherence length over which SHG is

produced in the non-phase-matchable material and, to a lesser extent, by the sample polycrystallinity. We estimate this DOF to be ≈1 μm. This is in comparison to the 100 nm DOF that is realized in the corresponding one-photon excited experiments, for which the DOF is limited by the penetration depth of the pump beam into the sample.
[30] S. K. Kurtz, T. T. Perry, *J. Appl. Phys.* **1968**, *39*, 3798 – 3813.
[31] TRSHG NSOM experiments using one-photon excitation were not feasible at the time of publication because 3.1 eV photons at the intensities required to observe TRSHG signals caused the SiO_2 NSOM fiber probe to luminesce over a broad spectral range. Two-photon sample excitation, however, did not cause this problem.
[32] C. L. Guo, G. Rodriguez, M. Hoffbauer, A. J. Taylor, *Appl. Phys. Lett.* **2001**, *78*, 3211 – 3213.
[33] R. Braun, B. D. Casson, C. D. Bain, E. W. M. van der Ham, Q. H. F. Vrehen, E. R. Eliel, A. M. Briggs, P. B. Davies, *J. Chem. Phys.* **1999**, *110*, 4634 – 4640.
[34] T. Kawai, D. J. Neivandt, P. B. Davies, *J. Am. Chem. Soc.* **2000**, *122*, 12031 – 12032.
[35] R. C. Dunn, *Chem. Rev.* **1999**, *99*, 2891 – 2927.

Received: July 14, 2003 [Z907]

Low Temperature Conductance Measurements of Self-Assembled Monolayers of 1,4-Phenylene Diisocyanide

Christian J.-F. Dupraz, Udo Beierlein, and Jörg P. Kotthaus*[a]

In the past few years, significant progress has been made in the fabrication and demonstration of molecular wires,[1–3] molecular diodes[4] and switches.[5] Many of these advances have been made possible by using the self-assembly of molecules on nanofabricated semiconductor and/or metallic structures. The most studied molecular system for electronic transport is the Au-SR system, where a self-assembled monolayer (SAM) of an oligomer (R) binds to a gold surface via a thiol group. In order to measure the electrical current through such a molecular layer, a second electrode is needed. This counterelectrode can be provided by an STM tip,[6–9] by another gold wire that can be approached using a mechanical break-junction[1, 10] or by evaporation of a gold layer on top of the SAM.[4] Other techniques employ electromigration of Au[11] or Au particles to achieve small interelectrode distances.[12] In spite of a growing number of publications dealing with electronic transport through molecules, even the conductance and transport mechanisms of relatively simple molecules are not well understood. The reasons lie in the difficulty of providing stable, well-defined metallic contacts at two ends of a molecule, which can allow reproducible transport measurements. It is the purpose of this paper to present two novel sample designs for conductance measurements which were applied to SAMs of the same molecule and to discuss the possible transport mechanisms involved.

One idea for implementing elementary molecular electronic computational functions requires the use of a three-terminal molecular-scale transistor.[13] To this day, only a small number of experiments showing field-effect behavior of molecules have been published.[11, 14, 15] One requirement for a transistor is that it exhibits signal gain which has not been achieved so far in molecular three-terminal devices. Another condition which has to be fulfilled in order to build a molecular field-effect transistors is a strong variation of the density of states (DOS) near the Fermi level of the molecules used. Ideally, the molecules should exhibit a very low conductance at off-resonance conditions and a high transmission in the case that the Fermi level is shifted electrostatically with a gate voltage to resonance. Lang and Avouris[16] have shown theoretically that 1,4-phenylene diisocyanide (PDC), the molecule used in this study, should meet this condition and would therefore be a good candidate for a field-effect device. Temperature-dependent conductance measurements were carried out by Chen et al.[17] with SAMs of PDC, which showed that both hopping and thermal emission of charge carriers could play a role in the conduction mechanisms involved.

Sample Preparation

Two novel fabrication techniques were employed to measure the conductance through a small area of self-assembled molecules.

Method A: Sandwich Architecture

For the first technique, highly p-doped Si with a top layer of 150 nm of SiO_2 was used as a substrate. Metal electrodes were fabricated by a combination of photolithography for the bonding pads and electron beam lithography for the patterning of the fine structures. A first electrode of typically 2 μm length and 200 nm width was defined by electron beam lithography, followed by the evaporation of 3 nm of NiCr and 50 nm of Au. This is followed by a liftoff in acetone and cleaning in ethanol (Figure 1 a, I). In the next step, the mask for a second electrode

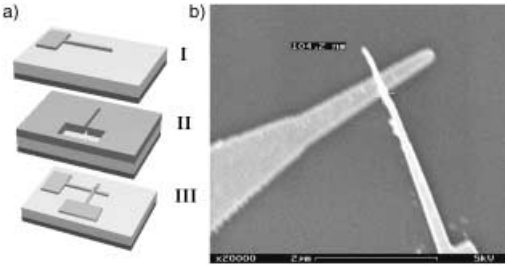

Figure 1. *a) Fabrication of samples of type A and b) SEM image of such a sandwich structure.*

[a] *Prof. Dr. J. P. Kotthaus, C. J.-F. Dupraz, Dr. U. Beierlein*
Center for NanoScience and Sektion Physik
Ludwig-Maximilians-Universität-München
Geschwister-Scholl-Platz 1, 80539 München (Germany)
Fax: (+49) 89 – 2180 – 3182
E-mail: udo.beierlein@physik.uni-muenchen.de

